

# PROCEEDINGS OF SPIE

SPIEDigitalLibrary.org/conference-proceedings-of-spie

## Assessment of 3D reconstructed image quality for computer-generated holographic 3D display

Tianshun Zhang, Yun Chen, Minjie Hua, Mingxin Zhou,  
Wenlong Zou, et al.

Tianshun Zhang, Yun Chen, Minjie Hua, Mingxin Zhou, Wenlong Zou,  
Jianhong Wu, "Assessment of 3D reconstructed image quality for computer-generated holographic 3D display," Proc. SPIE 12169, Eighth Symposium on Novel Photoelectronic Detection Technology and Applications, 12169B5 (27 March 2022); doi: 10.1117/12.2626597

**SPIE.**

Event: Eighth Symposium on Novel Photoelectronic Detection Technology and Applications, 2021, Kunming, China

# Assessment of 3D Reconstructed Image Quality for Computer-generated Holographic 3D Display

Tianshun Zhang<sup>a,b</sup>, Yun Chen<sup>a,b</sup>, Minjie Hua<sup>a,b</sup>, Mingxin Zhou<sup>a,b</sup>, Wenlong Zou<sup>a,b</sup> and Jianhong Wu<sup>\*a,b</sup>

<sup>a</sup>School of Optoelectronic Science and Engineering & Collaborative Innovation Center of Suzhou Nano Science and Technology, Soochow University, Suzhou 215006, China

<sup>b</sup>Key Lab of Advanced Optical Manufacturing Technologies of Jiangsu Province & Key Lab of Modern Optical Technologies of Education Ministry of China, Soochow University, Suzhou 215006, China

## ABSTRACT

A methodology of assessing a three-dimensional (3D) reconstructed image quality objectively for computer-generated holographic 3D display based on evaluating the reconstructed optical field is proposed. According to the concept of ‘holographic view-window’ (HVW), the point source method is used to calculate the ‘ideal’ Fresnel hologram and the precise diffraction field is numerically simulated after the 3D model is finely sampled. This accurate diffraction field is used as the evaluation criteria that can be regarded as ‘ground truth’. In comparison with the reconstructed images of the 3D diffraction field obtained by other common algorithms, such as point source method (PSM), Gerchberg-Saxton iterative (GS) algorithm and frequency-filtering method (FFM), the rationality of the evaluation function—the peak signal-to-noise ratio (PSNR) for the image quality assessment (IQA) of the 3D reconstructed diffraction field is investigated comprehensively at different reconstructed distances. The simulation results indicate that the PSNR is relatively reasonable for the evaluation of 3D reconstructed images taking into account the defocusing phenomena. The investigation would suggest an alternative optical scheme for the objective assessment of 3D image quality which provides a theoretical basis for the detection of holographic 3D image quality, the improvement of holographic 3D display algorithms and the design of the future spatial light modulator (SLM).

**Keywords:** computer-generated hologram, 3D display, image quality evaluation, precise diffraction field

## 1. INTRODUCTION

In the current market, people can experience and purchase an increasing number of mature 3D display devices and products such as 3D TVs, AR/VR head-mounted display devices, 3D games and videos, etc. which have all been favored by the public. Most of these devices or products are based on binocular parallax 3D display solutions, and the schemes for their IQA are gradually well-established [1-2]. For example, a series of 3D display databases like the existing LIVE 3D IQA database provides binocular disparity maps and depth maps of 3D objects that contain a variety of noise types, and provides subjective scores of stereoscopic images for the IQA. These standard datasets and subjective scores also provide a feasible basis for the objective evaluation of the imaging quality of the above-mentioned equipment.

Unlike the parallax display solution, the holographic 3D display, which is referred to as true 3D display, presents a real 3D reconstructed image that can essentially overcome the accommodation-convergence conflict [3]. So the holographic 3D display can be recognized as an ultimate solution among all the technical proposals for the 3D display, among which computer-generated hologram can not only record the amplitude and phase information of the object wave simultaneously but also calculate the hologram generated by the complex virtual model conveniently and flexibly. In the field of holographic applications, it is essential to objectively evaluate the influence of the distortion generated by the optical path and algorithms on the quality of the 3D image. However, compared with image quality evaluation schemes based on

---

<sup>\*</sup> jhwu@suda.edu.cn

disparity maps, there are relatively few schemes for holographic 3D displays. The current proposals are confined to subjective assessments consisting of qualitative [4] or quantitative analysis (such as Double Stimulus Impairment Scale, DSIS) [5-7], or merely objective approaches for 2D images [8-11]. For the 3D cases, the assessments generally only judge the result at a single focus distance, ignoring the effect of defocusing information on the different depth planes by observation or measurement, let alone the difficulty of experimental detection [12] and the lack of systematic explanation for the selection of evaluation criteria and functions [13]. Recently, researchers [14] used PSNR and Structural Similarity (SSIM) to evaluate the different depth planes of 3D images as a reference which are calculated by the look-up table method (LUT) with the entire PSF. The average of these values is used as the basis for evaluating the relative quality of different shapes and sizes of zone plates and different algorithms. The scheme is a worth considering method, but not universal.

Since there is no standard method for evaluating the quality of holographic 3D display, this paper proposes a full-reference method for objective 3D IQA based on optical diffraction field. From the perspective of IQA, the biggest difference between a 3D object and a 2D image is that the 3D image has two characteristics, scattering anisotropy and occlusion relationship. With the restricted viewpoint-based approach to IQA of a 3D object, the overall 3D IQA will be complicated and arduous. Instead, the solution based on the holographic view-window (HVW) can naturally solve these problems and can be easily detected by the array detector [15] as the complete 3D image with the above characteristics can be observed within the view-window range. Moreover, the difficulty lies in obtaining a benchmark while the full-reference evaluation is applied due to the lack of ground truth. The proposal based on HVW in this paper is to calculate the complex amplitude diffraction field of the 3D object after fine sampling. Then use the ‘ideal’ spatial light modulator (SLM) to load the hologram and the precise Fresnel diffraction field is reconstructed. Finally, the light intensity distribution at different focal planes in both accurate field and compared field can be compared pixel-by-pixel. Note that the SLM involved in the simulation calculation in this paper will be an ideal model capable of complex amplitude modulation and high enough resolution. The complex amplitude field actually can be achieved by algorithms or other methods [16-21] in reality.

## 2. 3D RECONSTRUCTED IMAGE EVALUATION SCHEME

### 2.1 Optical system

The optical path of a general holographic 3D display is portrayed in Figure 1, which is also an optical application scene for the 3D IQA proposed in this paper. The green laser with a wavelength of 532 nm passes through 2 polarizers and emits linearly polarized light with suitable intensity. After the laser beam is expanded and collimated, the beam direction is changed by the beam-splitting prism to vertically enter the effective area of the SLM (the number of pixels is  $1920 \times 1080$ , and the pixel size is  $8 \mu\text{m}$ ). The computer calculates the diffraction pattern of the 3D model on the hologram plane using different algorithms. The corresponding hologram is loaded on the ideal SLM which is able to modulate the complex amplitude of the incident light wave. The reconstructed Fresnel diffraction field is eventually obtained and passes through the field lens so as to be observed. A detector like CCD can also directly receive the light intensity signal without the field lens, hence the optical elements included in the figure are not necessary. Actually, the optical elements in a specific light path need to be added or removed depending on algorithms and applications. A reconstructed image generated by a ‘dinosaur’ model as an example is demonstrated in Figure 1.

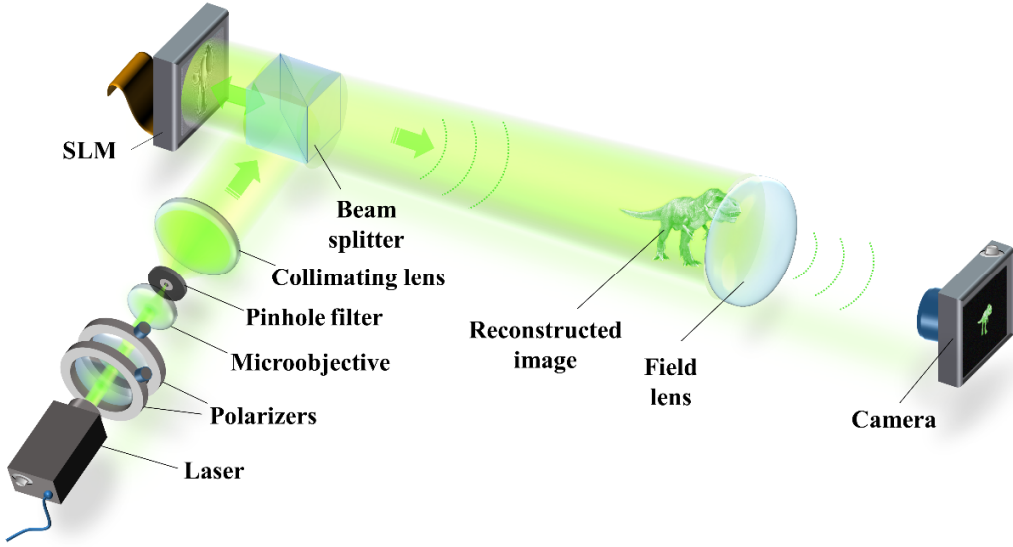


Figure 1. Schematic diagram of the 3D optical path for holographic 3D display.

## 2.2 Calculation method

The finely sampled model will be close to the original, whose diffraction field can be used as the comparison benchmark for the full-reference IQA. The light emitted by these object points reaches the hologram plane through Fresnel diffraction, and all the zone plates filled with the hologram are superimposed to form the hologram that needs to be loaded on the SLM [22]. Furthermore, when the maximum value of space-frequency  $F_{max}$  [23] of the carrier device SLM is considered, observers can see the complete image within a certain range which can be defined as HVW. When calculating the accurate diffraction field in this paper, an algorithm similar to T-FFT is used to speed up the calculation. The difference is that the impulse response is not approximated. The light field distribution of the hologram plane is calculated by the following formula:

$$U(p\Delta x, q\Delta y) = \sum \sum F^{-1} \left\{ F[U_0(m\Delta x, n\Delta y)] \cdot F \left[ \frac{1}{r} \exp[jkr] \right] \right\}_{r=\sqrt{(p\Delta x)^2 + (q\Delta y)^2 + z_0^2}} \quad (1)$$

$$(p, q, m, n = -N/2, -N/2+1, \dots, N/2-1)$$

where  $\Delta x = \Delta y = \text{pix}_2 = \frac{H_x}{M} = \frac{H_y}{N}$  represents the sampling length of hologram plane,  $Z_0$  is recording distance,  $\lambda$  represents the wavelength of light,  $j^2 = -1$ ,  $k = \frac{2\pi}{\lambda}$ .

The holographic algorithm needs to satisfy the sampling theorem in order to restore the signal of the object more truly. When the number of object sampling points increases and the sampling interval becomes smaller, for the sake of distinguishing the object points, the size of the hologram should be correspondingly larger, and meanwhile, the sampling interval of it should be small enough to separate the image spectrum islands. Suppose the pixel size of the object plane is  $\text{pix}_1$ , the number of pixels of the object plane is  $M_1 \times N_1$ , the pixel size of the holographic plane is  $\text{pix}_2$ , the number of

pixels is  $M_2 \times N_2$ , and the recording distance  $Z_0 = 300$  mm. According to the diffraction limit condition, the minimum aperture size  $W$  of the hologram can be obtained. It should be pointed out that the resolution limit of coherent illumination is slightly different from that of incoherent illumination in the constant factor, which is related to the shape of the object, the shape of the aperture and the sensitivity of the receiver [24]. Since the aperture of the holographic surface is always limited, only the minimum requirements are given here:

$$W = \frac{1.22\lambda \cdot z_0}{\text{Pix}_1} \quad (2)$$

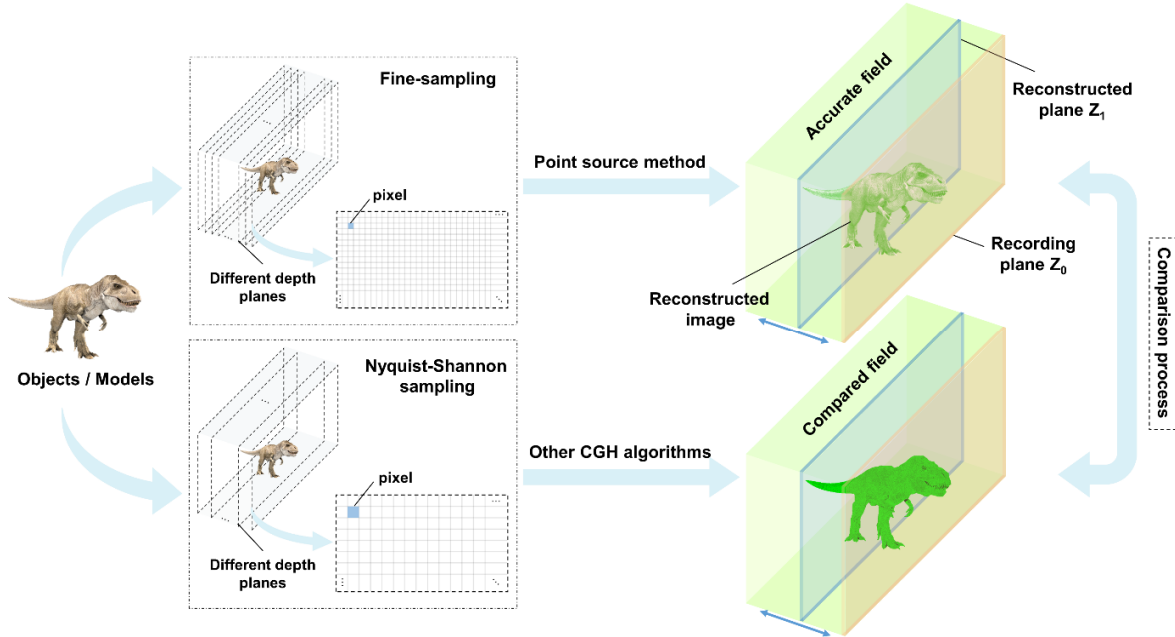


Figure 2. Flow chart of the 3D IQA scheme. The 3D object is sampled in two different ways to generate an accurate field and a compared field. As the recording distance (orange planes) is determined, the planes with corresponding reconstruction depths in the two diffraction fields are defined as the comparison plane pair (blue planes) which is compared.

As shown in Figure 2, a 3D object with a continuous surface is divided into different depth planes at a longitudinal sampling interval  $P_z$  and each depth plane is sampled again. The obtained dot matrix data is used to generate a corresponding hologram using a holographic algorithm. Finally, a 3D reconstructed image can be calculated numerically. When the above sampling conditions are met, the point source method is used to calculate an accurate 3D diffraction field that is close to the original and used as a benchmark. In this paper, the compared fields are calculated by some commonly used algorithms (such as point source method (PSM) [22], GS iteration [25], frequency domain filtering method (FFM) [23]), and the comparison between the 3D image and the 3D object is transformed into comparing two diffraction fields.

When the recording distance  $Z_0$  is determined, different reconstructed distances will produce different defocusing phenomena. The reconstructed plane is used as the compared plane, and both compared planes of the accurate field and the compared field move back and forth within a certain depth range. The overall light intensity distribution of these 2D plane pairs which contain the focus information at one certain depth and the defocus one at the other are compared. Therefore, the comparison of 3D light fields reduces the dimensionality of the 2D plane. In this paper, the PSNR [26] is used to evaluate the image quality of the 3D reconstructed image. The expression of PSNR is as follows:

$$PSNR = 10 \lg \frac{255^2}{\frac{1}{MN} \sum_{i=1}^M \sum_{j=1}^N |R_{z_1}(i, j) - O_{z_1}(i, j)|^2} \quad (3)$$

where M, N are the number of pixels in the X-Y direction,  $R_{z_1}(i, j)$  and  $O_{z_1}(i, j)$  respectively represent the 2D image at the reconstructed distance in the compared field and the accurate field. Higher PSNR indicates better image quality. In other words, the image of the comparison field is closer to the ground truth.

### 3. SIMULATION RESULTS AND DISCUSSION

#### 3.1 Determination of the accurate field

The goal of accurate field design is that the number of sampling points for the object should be large and the sampling interval should be small enough under the condition of the unchanged real size of the object. In practical applications, the accurate field can be determined by the actual compared field. The following calculations for both compared field and accurate field algorithms are all PSMs, and the calculated holograms are all directly reconstructed with complex amplitude. For the 3D model ‘dinosaur’, the following 5 kinds of accurate field sampling conditions are made. As shown in Figure 3 (a), the resolutions of the object are  $2400 \times 1350$ ,  $3072 \times 1728$ ,  $3840 \times 2160$ ,  $6144 \times 3456$ ,  $7680 \times 4320$ . Early simulation results show that the vertical sampling interval also has a certain impact on image quality, whereas considering that the human eye is far less sensitive to the vertical resolution than the horizontal one [27]. The vertical sampling interval  $P_z$  for the accurate field and the compared field are both 0.05 mm. The actual size of the 3D model remains unchanged, so the sampling interval becomes smaller and the total number of sampling points increases.

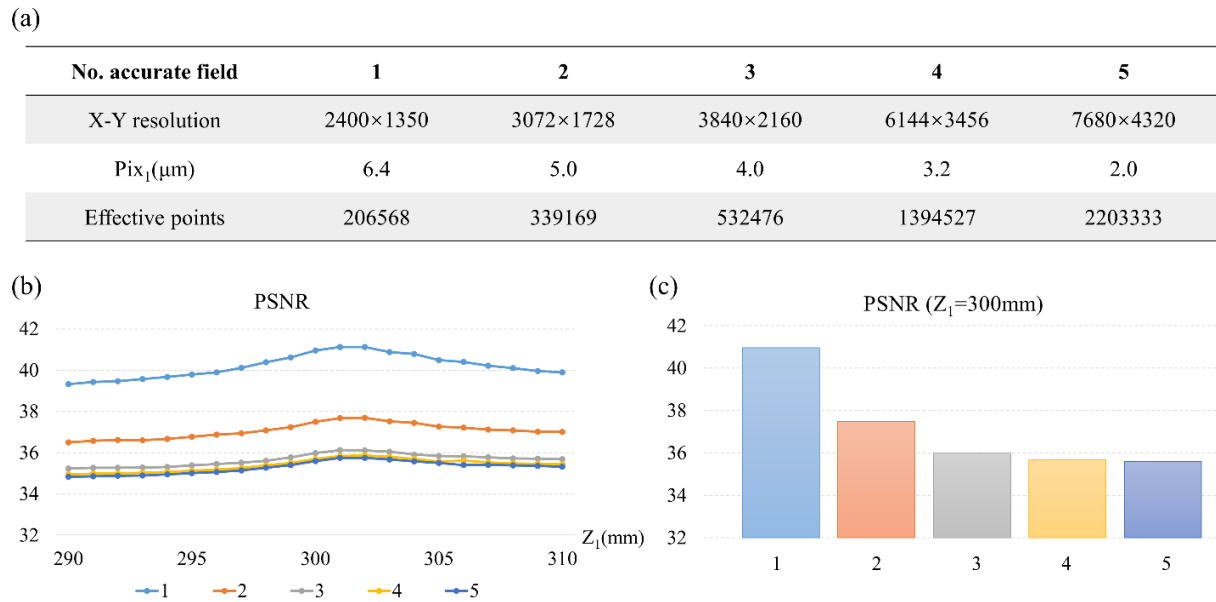


Figure 3. (a) The parameters of five accurate field models. (b) The PSNR curves of different accurate field sampling models. (c) The PSNR histograms of different accurate field models at the reconstructed distance  $Z_1=300\text{mm}$ .

When the compared field remains unchanged (the resolution is  $1920 \times 1080$ , the sampling interval is  $8 \mu\text{m}$  and the number of dinosaur model points is 131998), the accurate field uses the above five sampling models. The comparison plane  $Z_1$  is 300 mm, and the focus is on the head of the dinosaur model. The evaluation function PSNR is calculated, when the

recording distance  $Z_0 = 300$  mm and the reconstructed distance range  $Z_1$  is within the range of 290 mm - 310 mm. As shown in Figure 3 (b), it indicates that, with the gradual refinement of the sampling, the PSNRs gradually become smaller and tend to converge. For the same accurate field model, the PSNR curve fluctuates slightly due to the influence of the spatial point distribution of the 3D model. Figure 3 (c) gives an example of the reconstructed distance. Taking into account the balance between calculation cost and image quality improvement, it can be considered that after Model 5, the accuracy level meets the demand. The accurate field selected is Model 5 hereinafter.

### 3.2 Results of 3D model comparison

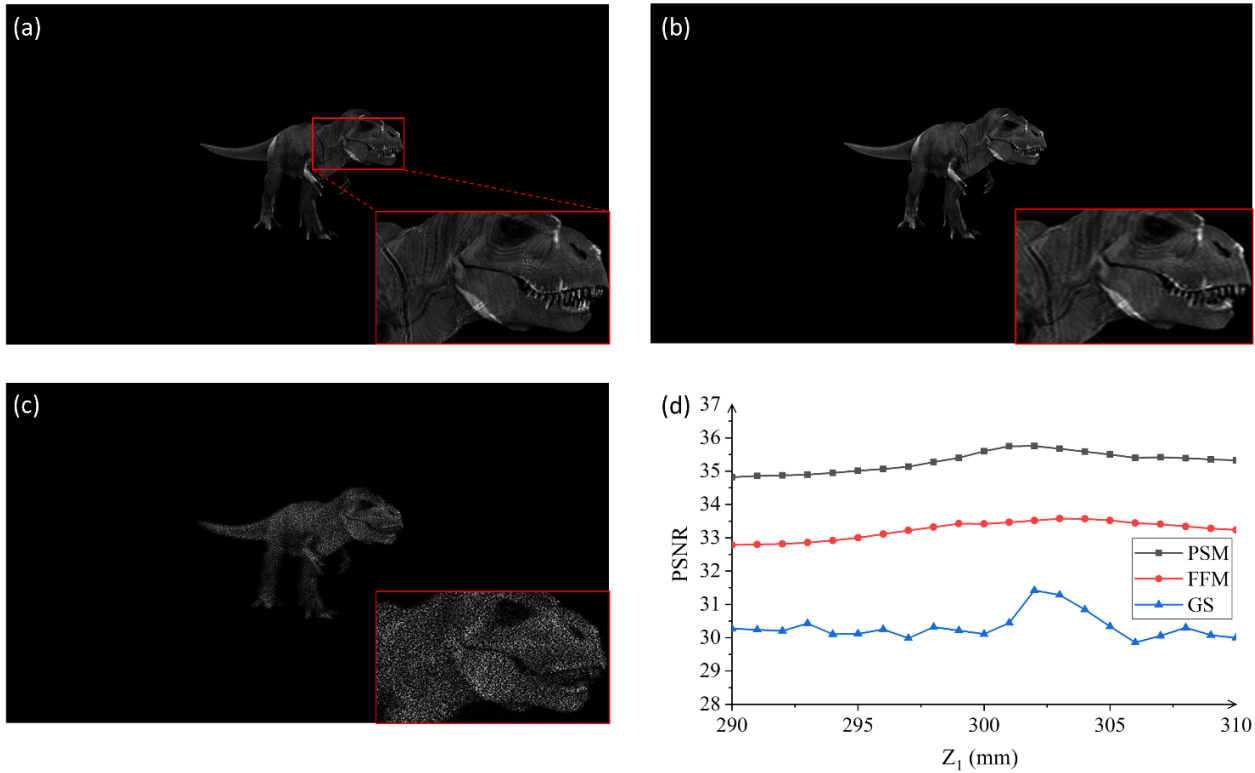


Figure 4. (a) - (c) are respectively the normalized light intensity simulation results and partially enlarged diagrams calculated by the point source method, frequency domain filtering method and GS algorithm at the reproduction distance  $Z_1 = 300$  mm. (d) is the PSNR curve of different algorithms within a certain range of reproduction distance.

Next, the situation of different algorithms in the 3D model is explored. The compared plane scans with a step length of 1 mm within the range of 290 mm-310 mm. The horizontal resolution of the 3D model is 1920×1080, and the vertical sampling interval  $P_z$  is 0.05 mm. Figures 4 (a) - (c) show respectively the normalized light intensity simulation results and partially enlarged diagrams at  $Z_1 = 300$  mm calculated by PSM with complex amplitude, FFM and the GS algorithm. This situation is similar to the previous work of our research group [23] when the compared field calculation algorithm was selected as the FFM. The difference is that the zone plates calculated in this paper fill the entire hologram plane instead of being band-limited, while the intensity modulation factor  $\gamma$  still affects the diffraction efficiency and image quality. According to the conclusion of previous work, as  $\gamma$  increases, the image quality deteriorates and the diffraction efficiency increases, so the choice of  $\gamma$  is the result of a trade-off. Therefore, the FFM here selects the result when  $\gamma = 1$ . According to the proposed IQA scheme, the PSNR result curves of these algorithms at different reconstructed distances are calculated.

As shown in Figure 4 (d), the three curves do not intersect with each other, and the PSNR of the arbitrary plane within the given range can characterize the image quality calculated by each algorithm. The PSNR of the PSM > FFM > GS algorithm. This range is related to the selection of specific models, and the result is consistent with the subjective perception of the human eye as shown in Figure 4 (a) - (c).

#### 4. CONCLUSION

This paper proposes a 3D IQA scheme based on the diffraction field for holographic 3D displays. The accurate field with the HVW of the 3D object is calculated and determined, which is used as a benchmark for comparison. The compared field obtained by the point source method, GS algorithm, and frequency domain filtering method is compared with the light intensity distribution at different reconstructed planes, and the corresponding PSNR is calculated. It is found that within a certain range of reconstructed distance, the image quality can be evaluated reasonably by comparing the PSNR of any plane. Moreover, the simulation result is the same as the subjective perception of the human eye, and it provides an alternative scheme and theoretical basis for the IQA of the 3D reconstructed image for future researchers engaged in holographic 3D display. Due to the lack of a standard and unified 3D holographic database and subjective score set of human eyes, the evaluation needs to be further improved. In the future, the applicability of more 3D models and evaluation functions needs to be further verified, and the detectability in experimental measurement can be explored.

#### ACKNOWLEDGEMENTS

This work is supported by Priority Academic Program Development of Jiangsu Higher Education Institutions.

#### REFERENCES

- [1] Moorthy A. K., Su C. C. and Mittal A., "Subjective evaluation of stereoscopic image quality," *Signal Process Image Commun.*, 28(8), 870-883 (2013).
- [2] Yoshikawa, H., Yamaguchi, T. and Uetake, H., "Image quality evaluation and control of computer-generated holograms," *Proc. SPIE* 9771, p.97710N (2016).
- [3] Jason and Geng, "Three-dimensional display technologies," *Adv. Opt. Photon.*, 5(4), 456–535 (2013).
- [4] Kozacki, T., Martinez-Carranza, J. and Kukolowicz, R., "Accurate reconstruction of horizontal parallax-only holograms by angular spectrum and efficient zero-padding," *Appl. Opt.*, 59(27), 8450-8458 (2020).
- [5] Ahar, A., Blinder, D. and Bruylants, T., "Subjective quality assessment of numerically reconstructed compressed holograms," *International Society for Optics and Photonics*, 9599, 95990K (2015) .
- [6] Amirpourazarian, H., Pinheiro, A., Fonseca, E., Ghanbari, M. and Pereira, M., "Quality evaluation of holographic images coded with standard codecs," *IEEE Trans Multimedia*, 10(1109), 3096059 (2021).
- [7] Lehtimäki, T. M. and Taina, M., "Evaluation of perceived quality attributes of digital holograms viewed with a stereoscopic display," *IEEE 2010 9th Euro-American Workshop on Information Optics*, 1–3 (2010).
- [8] Choi, S., Kim, J., Peng, Y. and Wetzstein, G., "Optimizing image quality for holographic near-eye displays with michelson holography," *Optica*, 8(2), 143-146 (2021).
- [9] Yoshikawa, H. and Yamaguchi, T., "Image Quality Evaluation of a Computer-Generated Hologram," *Optical Society of America, In Digital Holography and Three-Dimensional Imaging*, DT2A-8 (2015).
- [10] Yoshikawa, H., Yamaguchi, T. and Uetake, H., "Image quality evaluation and control of computer-generated holograms," *International Society for Optics and Photonics, Practical Holography XXX: Materials and Applications.*, 9771: 97710N (2016).
- [11] Qu, W., Gu, H. and Tan, Q., "Holographic projection with higher image quality," *Opt. Express*, 24(17), 19179-19184 (2016).
- [12] Horisaki, R., Takagi, R. and Tanida, J., "Deep-learning-generated holography," *Appl. Opt.*, 57(14), 3859 (2018).
- [13] Zhou, W., Bovik, A. C. and Sheikh, H. R., "Image quality assessment: from error visibility to structural similarity,"

- IEEE Trans Image Process, 13(4) (2004).
- [14] Yasuki, D., Shimobaba, T., Makowski, M., Suszek, J., Kakue, T. and Ito, T., "Hologram computation using the radial point spread function," *Appl. Opt.*, 60(28), 8829-8837 (2021).
- [15] Chao, Z., Xiaolei, Z., Yan, H., Wei, Y., Detong, S., Jinxin, Z. and Qian, C., "Has 3D finally come of age?—An introduction to 3D structured-light sensor," *Infrared and Laser Engineering*, 49(3), 0303001 (2020).
- [16] Li, X., Liu, J. and Jia, J., "3D dynamic holographic display by modulating complex amplitude experimentally," *Opt. express*, 21(18), 20577-20587 (2013).
- [17] Gao, Q., Liu, J. and Han, J., "Monocular 3D see-through head-mounted display via complex amplitude modulation," *Opt. Express*, 24(15), 17372–17383 (2016).
- [18] Gao, Q., Liu, J. and Duan, X., "Compact see-through 3D head-mounted display based on wavefront modulation with holographic grating filter," *Opt. Express*, 25(7), 8412–8424 (2017).
- [19] Zhang, Z., Liu, J. and Duan, X., "Enlarging field of view by a two-step method in a near-eye 3D holographic display," *Opt. Express*, 28(22), 32709–32720 (2020).
- [20] Choi, S., Kim, J. and Peng, Y., "Optimizing image quality for holographic near-eye displays with Michelson Holography," *Optica*, 8(2), 143–146 (2021).
- [21] Song, W., Li, X., Zheng, Y., Liu, Y. and Wang, Y., "Full-color retinal-projection near-eye display using a multiplexing encoding holographic method," *Opt. Express*, 29(6), 8098–8107 (2021).
- [22] Zhang, H., Collings, N., Chen, J., Crossland, B., Chu, D. and Xie, J. H., "Full parallax three-dimensional display with occlusion effect using computer generated hologram," *Opt. Eng.* 50(7), 074003-074003-5 (2011).
- [23] Chen, Y., Hua, M., Zhang, T., Zhou, M., Wu, J. and Zou, W., "Holographic near-eye display based on complex amplitude modulation with band-limited zone plates," *Opt. Express*, 29(14), 22749-22760 (2021).
- [24] Born, M. , Clemmow, P. C. , Gabor, D. , Stokes, A. R. , Taylor, A. M. and Wayman, P. A. , Principles of optics. Pergamon Press (1959).
- [25] Gerchberg, R. W., "A practical algorithm for the determination of phase from image and diffraction plane pictures," *Optik*, 35, 237-246 (1972).
- [26] Hontsch, I. and Karam, L. J., "Locally adaptive perceptual image coding," *IEEE Trans. On Image Processing*, 9(9), 1472-1483 (2000).
- [27] Wang, Z., Bovik, A. C., Sheikh, H. R. and Simoncelli, E. P., "Image quality assessment: From error visibility to structural similarity," *IEEE Trans. On Image Processing*, 13(4), 600-612 (2004).